Myeloid Malignancies with Chromosome 5q Deletions Acquire a Dependency on an Intrachromosomal NF-κB Gene Network

Article *in* Cell Reports · September 2014

DOI: 10.1016/j.celrep.2014.07.062 · Source: PubMed

CITATIONS
7

READS
53

15 authors, including:

Xiaona Liu
Cincinnati Children's Hospital Medical Center
11 PUBLICATIONS **158** CITATIONS
SEE PROFILE

Dinesh S Rao
University of California, Los Angeles
74 PUBLICATIONS **5,202** CITATIONS
SEE PROFILE

H. Leighton Grimes
Cincinnati Children's Hospital Medical Center
104 PUBLICATIONS **4,815** CITATIONS
SEE PROFILE

Matthew T Weirauch
Cincinnati Children's Hospital Medical Center
157 PUBLICATIONS **6,253** CITATIONS
SEE PROFILE

OPEN ACCESS
CellPress

Cell Reports
Report

Myeloid Malignancies with Chromosome 5q Deletions Acquire a Dependency on an Intrachromosomal NF-κB Gene Network

Jing Fang,[1] Brenden Barker,[1] Lyndsey Bolanos,[1] Xiaona Liu,[1] Andres Jerez,[2] Hideki Makishima,[2] Susanne Christie,[1] Xiaoting Chen,[3,4] Dinesh S. Rao,[5] H. Leighton Grimes,[1,6] Kakajan Komurov,[1] Matthew T. Weirauch,[3,7] Jose A. Cancelas,[1,8] Jaroslaw P. Maciejewski,[2] and Daniel T. Starczynowski[1,9,*]

[1]Division of Experimental Hematology and Cancer Biology, Cincinnati Children's Hospital Medical Center, Cincinnati, OH 45229, USA
[2]Department of Translational Hematology and Oncology Research, Taussig Cancer Institute, Cleveland Clinic, Cleveland, OH 44195, USA
[3]Center for Autoimmune Genomics and Etiology (CAGE), Cincinnati Children's Hospital Medical Center, Cincinnati, OH 45229, USA
[4]Department of Electrical Engineering and Computing Systems, University of Cincinnati, Cincinnati, OH 45229, USA
[5]Department of Pathology and Laboratory Medicine, UCLA, Los Angeles, CA 90095, USA
[6]Division of Immunobiology, Cincinnati Children's Hospital Medical Center, Cincinnati, OH 45229, USA
[7]Divisions of Biomedical Informatics and Developmental Biology, Cincinnati Children's Hospital Medical Center, Cincinnati, OH 45229, USA
[8]Hoxworth Blood Center, University of Cincinnati College of Medicine, Cincinnati, OH 45219, USA
[9]Department of Cancer Biology, University of Cincinnati College of Medicine, Cincinnati, OH 45267, USA
*Correspondence: daniel.starczynowski@cchmc.org
http://dx.doi.org/10.1016/j.celrep.2014.07.062

SUMMARY

Chromosome 5q deletions (del[5q]) are common in high-risk (HR) myelodysplastic syndrome (MDS) and acute myeloid leukemia (AML); however, the gene regulatory networks that sustain these aggressive diseases are unknown. Reduced miR-146a expression in del(5q) HR MDS/AML and miR-146a$^{-/-}$ hematopoietic stem/progenitor cells (HSPCs) results in TRAF6/NF-κB activation. Increased survival and proliferation of HSPCs from miR-146a^{low} HR MDS/AML is sustained by a neighboring haploid gene, *SQSTM1* (*p62*), expressed from the intact 5q allele. Overexpression of *p62* from the intact allele occurs through NF-κB-dependent feedforward signaling mediated by miR-146a deficiency. p62 is necessary for TRAF6-mediated NF-κB signaling, as disrupting the p62-TRAF6 signaling complex results in cell-cycle arrest and apoptosis of MDS/AML cells. Thus, del(5q) HR MDS/AML employs an intrachromosomal gene network involving loss of miR-146a and haploid overexpression of p62 via NF-κB to sustain TRAF6/NF-κB signaling for cell survival and proliferation. Interfering with the p62-TRAF6 signaling complex represents a therapeutic option in miR-146a-deficient and aggressive del(5q) MDS/AML.

INTRODUCTION

Deletions involving the long arm of chromosome 5 (chr5), del(5q), are the most common cytogenetic abnormalities in myelodysplastic syndrome (MDS) and secondary acute myeloid leukemia (AML) (Ebert, 2009). 5q− syndrome, a clinical entity defined by an isolated del(5q) with a blast count of <5%, confers a favorable prognosis and responsiveness to lenalidomide (Greenberg et al., 2012; List et al., 2006). However, a large proportion of del(5q) patients have bone marrow (BM) blasts exceeding 5%, complex cytogenetics, and extremely poor prognosis and are refractory to available treatments (Giagounidis et al., 2006). Minimally deleted regions (MDRs) have been mapped and extensively studied (Ebert, 2009). The distal MDR (5q33.3) on chromosome 5q (chr5q) is associated with a favorable outcome, while the proximal MDR (5q31.1) is associated with worse prognosis and leukemic transformation. More recently, high-resolution genomic analyses on an extensive patient cohort has added new insight into the clinical and genomic correlates of del(5q) myeloid malignancies. It was shown that the extent of the deleted region on 5q determines clinical characteristics (Jerez et al., 2012); that is, chr5q deletions extending beyond q34 portend a worse overall survival and are associated with high-risk (HR) disease. One potential candidate on chr5q is miR-146a, a microRNA (miRNA) implicated in del(5q) MDS/AML pathogenesis, which resides on band q34. From previous work, a subset of miR-146a$^{-/-}$ mice develop MDS, a myeloid proliferative disease, and/or myeloid tumors resembling AML, in part by derepression of tumor necrosis factor receptor-associated factor 6 (TRAF6) and persistent NF-κB activation (Boldin et al., 2011; Starczynowski et al., 2010; Zhao et al., 2011, 2013). The mechanism accounting for the variable phenotype and disease latency of miR-146a$^{-/-}$ mice is still unresolved, particularly as it relates to disease initiation versus disease maintenance. In addition, a small-molecule inhibitor of IRAK1 suppresses TRAF6 and NF-κB activation and induces apoptosis of primary MDS-propagating cells but is less effective as a single agent in primary AML (Rhyasen et al., 2013). Therefore, understanding the contribution of miR-146a deficiency to the maintenance of HR MDS/AML and uncovering novel therapeutic opportunities is warranted.

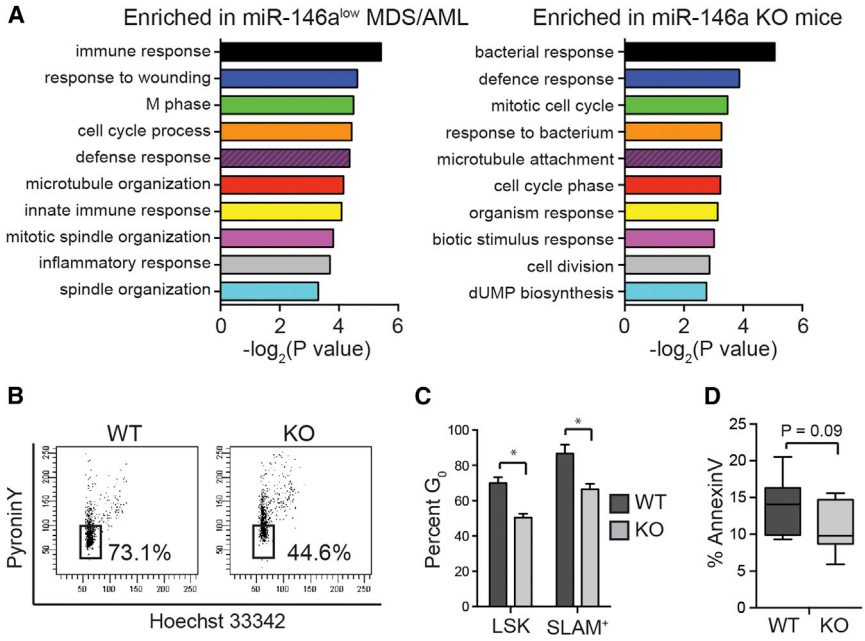

Figure 1. miR-146a Deletion Mediates HSPC Hyperproliferation

(A) Overexpressed genes from low miR-146a-expressing del(5q) MDS/AML patients and miR-146a$^{-/-}$ (KO) marrow cells were compared using ToppGene.

(B and C) Cell-cycle analysis was performed on Lin$^-$Sca-1$^+$cKit$^+$ (LSK) and SLAM$^+$ cells from WT (n = 4) and KO (n = 6) mice by Pyronin Y/Hoechst 33342 staining. Shown is a representative plot for LSK (B) and summary for LSK and SLAM$^+$ cells (C). *p < 0.05.

(D) Annexin V staining was performed on Lin$^-$cKit$^+$ cells from WT (n = 4) and KO (n = 6) mice.

See also Figure S1 and Table S1.

RESULTS

Loss of miR-146a expression either by miRNA decoy or by genetic deletion in mouse hematopoietic stem/progenitor cells (HSPCs) results in features of 5q− syndrome, fatal myeloid malignancies, and altered hematopoietic proportions (Figures S1A–S1F) (Boldin et al., 2011; Zhao et al., 2011, 2013); however, the effects of miR-146a loss that explain the clinical findings and sustained malignant cell growth in aggressive/HR del(5q) MDS/AML are not known. To investigate a connection between miR-146a loss and the cellular phenotype of del(5q) MDS/AML cells, gene expression patterns and Gene Ontology (GO) categories using ToppGene (Chen et al., 2009) were compared between HSPCs from miR-146a^{low} del(5q) MDS/AML patients (Table S1) and miR-146a$^{-/-}$ mice. The expression of miR-146a in this subset of del(5q) MDS/AML patients, which is ~80% lower as compared to age-matched controls, is best approximated by miR-146a$^{-/-}$ mice for functional comparisons as miR-146a expression in miR-146$^{+/-}$ (Het) BM cells is similar to wild-type (WT) mice (Figures S1A and S1G). The overlapping pathways were nearly identical between the two groups, which included overexpression of cell cycle, innate immune response, and survival pathway genes (Figure 1A). In support of the gene expression patterns, hematopoietic stem cells (HSCs) from miR-146a$^{-/-}$ mice have increased Pyronin Y (Figures 1B and 1C) and reduced Annexin V staining (Figure 1D; p = 0.09), suggesting that miR-146a-deficient HSCs are less quiescent and have increased survival. Consistent with increased HSPC proliferation and survival, miR-146$^{-/-}$ mice exhibit myeloid expansion (increased CD11b$^+$ cells as compared to WT HSPCs; Figures S1D and S1E) and impaired competitive engraftment (reduced CD45.2% chimerism in the peripheral blood; Figure S1F). As reported previously (Boldin et al., 2011; Starczynowski et al., 2010; Taganov et al., 2006), loss of miR-146a in leukemic cells results in derepression of TRAF6, a mediator of NF-κB activation (Figures S1H–S1K), implicating this molecular complex in the aggressive nature of the del(5q) MDS/AML phenotype.

Inhibiting the TRAF6/NF-κB axis may represent a therapeutic opportunity for aggressive forms of del(5q) MDS/AML with low miR-146a expression. Unfortunately, the success of direct inhibitors of NF-κB for human cancers has yet to be proven. Chromosome deletions that target tumor suppressor genes also involve multiple neighboring genes, such as with del(5q), and loss of certain neighboring genes may expose cancer-specific vulnerabilities and potential therapeutic targets (Muller et al., 2012; Nijhawan et al., 2012). To overcome the limitations of NF-κB inhibitors and identify novel mechanisms of disease dependency, we examined the expression of all genes residing within chr5q from del(5q) and control CD34$^+$ cells (Figure S2A). Of 1,528 chr5q genes, 374 genes were significantly lower (<0.5-fold) and 27 were higher (e.g., overexpressed/restored from the intact allele >1.5-fold) in del(5q) cells (Figure 2A; Table S2). We also examined the 27 overexpressed genes in non-del(5q) MDS (Figure S2B). Interestingly, a subset of these genes were also overexpressed in non-del(5q) MDS, but not to the same extent as in del(5q) MDS (Figure S2C). In addition, we utilized GeneConnector functionality in NetWalker to build molecular networks (Figure S2A) (Komurov et al., 2012). A single major "NF-κB" molecular node and a minor node related to "coagulation response" formed corresponding to the overexpressed chr5q genes (Figure 2B). To determine whether the "NF-κB node" is important for the proliferative phenotype in aggressive del(5q) MDS/AML, human leukemic and normal CD34$^+$ cells were treated with an NF-κB inhibitor (BAY 11-7085) and then analyzed for cell-cycle kinetics and viability. Following treatment with BAY 11-7085 or by knockdown of *TRAF6*, all MDS/AML cells exhibited a G2/M arrest and apoptosis (Figures S2D–S2H). In addition, miR-146a$^{-/-}$ HSPCs were more sensitive to NF-κB pathway inhibition by BAY 11-7085 than WT HSPCs, as evident by enhanced G2/M arrest (Figure S2G) and apoptosis (Figure S2I). These findings indicate that human and mouse miR-146a^{low} HSPCs are sensitive to genetic and pharmacologic inhibition of the TRAF6/NF-κB pathway, suggesting an acquired dependency on TRAF6.

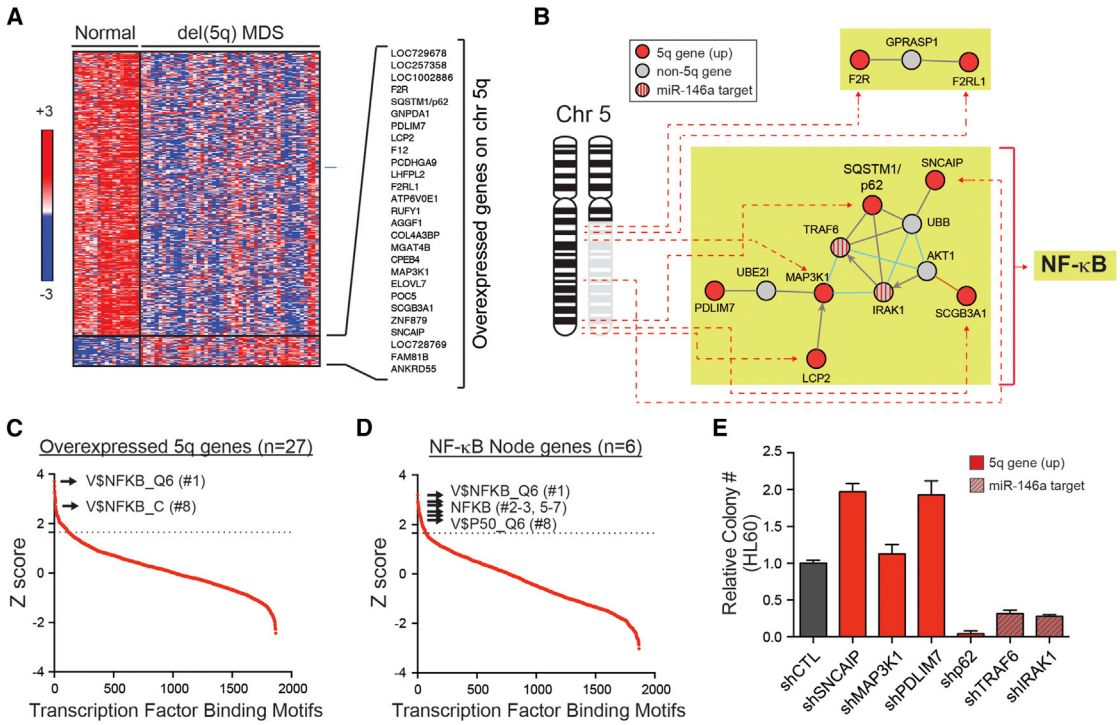

Figure 2. Del(5q) MDS/AML Are Associated with an Intrachromosomal NF-κB Feedforward Gene Network

(A) Gene expression profiling of differentially expressed chr5q genes (q11–q35) in del(5q) MDS (n = 47) as compared to normal control CD34$^+$ cells (n = 17).

(B) GeneConnector functionality in NetWalker was used to build a molecular network of genes that are overexpressed in del(5q) MDS (see Table S2 for all genes used in the analysis). Red nodes indicate genes overexpressed in del(5q) MDS. Gray nodes indicate molecularly connected genes. Gray nodes with red stripes indicate validated miR-146a gene targets. Dotted lines indicate the chromosome position of each gene.

(C and D) Enrichment scores for DNA binding motifs in the promoter regions of overexpressed 5q genes (C) and NF-κB node genes (D). Each point represents the enrichment *Z* score for a single transcription factor (TF) binding motif. Enriched motifs for NF-κB are indicated with arrows, along with their overall rank among the 1,867 total human TF motifs analyzed. Horizontal dashed line indicates the (uncorrected) significance threshold corresponding to a p value cutoff of 0.01 (see Table S3).

(E) Knockdown of *SNCAIP*, *MAP3K1*, *PDLIM7*, *p62*, *TRAF6*, and *IRAK1* in HL60 cells was achieved by shRNAs. Solid red histograms represent genes within the "NF-κB node" that reside on chr5q. Hatched red histograms represent genes within the NF-κB node that do not reside on chr5q (see Figure 2B). Transduced HL60 cells were evaluated for colony formation in methylcellulose following knockdown of each indicated gene. Colonies were scored and normalized to a control shRNA. $p < 0.05$ for HL60 cells transduced with shp62, shTRAF6, and shIRAK1.

See also Figure S2 and Tables S2 and S3.

Given the paradoxical overexpression of genes from the intact chr5 allele, we hypothesized that the 27 overexpressed genes might be coregulated by a common transcription factor (TF). We compiled a data set containing 1,867 DNA binding motifs representing the binding preferences of 623 human TFs to search for enriched TF binding sites in the promoter regions of the 5q overexpressed genes (Zambelli et al., 2009). Of all TF motifs, NF-κB binding sites are the most strongly enriched in the entire overexpressed/compensated gene set (Figure 2C; p = 0.0001) and even further enriched in the NF-κB node gene set (Figure 2D; p = 0.0007) (Table S3). To further explore the broader regulation of NF-κB-target gene expression, we examined two canonical NF-κB gene targets in normal CD34$^+$, del(5q) MDS, and non-del(5q) MDS. Despite the enrichment of NF-κB binding sites in a subset of genes residing on chr 5q, not all NF-κB-regulated genes are overexpressed in del(5q) MDS (Figure S2C). To determine which genes within the NF-κB node are necessary for del(5q) leukemic cell function, we knocked down the expression of each gene and examined leukemic progenitor function (Figure 2E). Based on previous reports, knockdown of *TRAF6* or *IRAK1* significantly impaired HL60 colony formation (Figure 2E). Of the genes within the NF-κB node that reside on chr5q, only knockdown of sequestosome 1 (*SQSTM1/p62*) resulted in reduced colony formation. Knockdown of the remaining NF-κB node genes did not result in impaired leukemic progenitor function, suggesting these genes are not sufficient to sustain the NF-κB-mediated survival signal. Among the overexpressed genes residing on chr5q and within the NF-κB node, *p62* (5q35, p = 0.0054; adjusted p = 0.023) emerged as an obvious candidate (Table S2), as it is required for leukemic progenitor function and is a cofactor for NF-κB activation through recruitment of TRAF6 (Duran et al., 2008; Linares et al., 2011; Moscat and Diaz-Meco, 2009; Wooten et al., 2005).

miR-146a regulates several genes within the innate immune pathway; however, an analysis of the 3′ UTR of *p62* did not reveal miR-146a binding sites, suggesting an alternative mechanism of

p62 overexpression in miR-146a^{low} cells. Examination of the *p62* promoter region using ENCODE functional genomics data (Rosenbloom et al., 2013) revealed the presence of two NF-κB (p50) chromatin immunoprecipitation sequencing (ChIP-seq) binding peaks (κB site motif: NGGGACTTTCCN) (Chen et al., 1998) in hematopoietic cells (Figure 3A). Both NF-κB binding motifs directly overlap DNase I-hypersensitive, H3K4 mono- and trimethylation, and H3K27 acetylation regions in hematopoietic/leukemic cells, reaffirming the prediction analysis (Figure 2) and confirming that NF-κB also binds these regions in leukemic cells. Therefore, these analyses suggest that NF-κB transcription factors regulate a subset of overexpressed genes on chr5q, one of which (*p62*) is a signaling mediator of the canonical NF-κB pathway. Analysis of an independent cohort of patients revealed that *p62* expression inversely correlated with miR-146a expression in HR del(5q) MDS/AML ($p = 0.013$; Figure 3B). Consistent with RNA expression in primary MDS/AML cells, p62 protein is expressed at normal or even at elevated levels despite deletion of one *p62* locus in certain MDS/AML samples and cell lines (Figure 3C; Figure S3). To further examine the molecular relationship among miR-146a, NF-κB, and p62, additional knockdown of miR-146a resulted in elevated p62 expression following interleukin-1β (IL-1β)-mediated (TRAF6-dependent) NF-κB activation, but not with tumor necrosis factor α stimulation (TRAF6 independent) (Figure 3D). Similarly, miR-146a$^{-/-}$ marrow cells exhibit elevated *p62* mRNA and protein expression following IL-1β-induced NF-κB activation (Figures 3E and 3F). We sought to investigate whether compensation of *p62* in this subset of del(5q) MDS/AML modified clinical outcome. Del(5q) MDS/AML patients were divided into miR-146a^{low}/*p62*^{high} and miR-146a^{high}/*p62*^{low} cohorts. Based on this stratification, del(5q) MDS/AML with miR-146a^{low}/*p62*^{high} had a significantly worse overall survival (Figure 3G; $p = 0.0064$), further implicating p62 as an essential cofactor in aggressive forms of del(5q) MDS/AML.

We next determined the function of p62 in miR-146a^{low}-expressing HSPCs. Overexpression of *p62* in miR-146a$^{-/-}$ HSPCs further increased cell proliferation as the proportion of cells in S phase increased and the proportion in G2/M decreased, whereas overexpression of p62 did not affect WT HSPCs (Figure 3H). Conversely, knockdown of *p62* in miR-146a$^{-/-}$ HSPCs (Figure 3I) reversed the proliferative phenotype by arresting cells in G2/M (Figures 3J and 3K). However, knockdown of *p62* in WT HSPCs resulted in minor changes in cell-cycle progression (Figures 3J and 3K). Since transplantation of miR-146a$^{-/-}$ BM results in diminished competitive myeloid reconstitution in recipient mice (Figure S1F), we evaluated whether knockdown of *p62* can restore these cellular consequences. As expected, knockdown of *p62* in WT HSPC did not alter proportions of CD11b^{+} or CD3^{+} cells, while transplantation of miR-146a$^{-/-}$ HSPCs transduced with control small hairpin RNA (shCTL) resulted in diminished myeloid reconstitution in recipient mice (Figure 3L). In contrast, knockdown of *p62* in miR-146a$^{-/-}$ HSPCs restored normal proportions of CD11b^{+} cells (Figure 3L; $p = 0.04$). Therefore, p62 is essential in miR-146a^{low}-expressing premalignant mouse HSPCs by regulating cell-cycle progression and myeloid cell development.

p62 is essential in certain solid tumors (Duran et al., 2008; Ling et al., 2012); therefore, we investigated whether p62 serves a similarly essential role in human myeloid malignancies. Utilizing lentiviral vectors encoding small hairpin RNAs (shRNAs) targeting *p62* (Figure S4A), knockdown of *p62* significantly reduced TRAF6 activation by ~75%, as measured by K63-linked autoubiquitination, in two human del(5q) MDS/AML cell lines (Starczynowski et al., 2011) (Figure 4A). Knockdown of *p62* also resulted in impaired NF-κB/p65 nuclear localization, but only following loss of miR-146a (Figure 4B). To examine the effects of p62 depletion in vivo, the MDS/AML cell lines were transduced with shp62 or control (shCTL) and then xenografted into nonobese diabetic *scid* gamma (NSG) mice. By 6–7 weeks, control leukemic cells expanded ~8-fold in the peripheral blood, while leukemic cells with *p62* knockdown did not expand and remained below 10% chimerism (Figure 4C). Mice with HL60 or MDS-derived cell line (MDSL) xenografts expressing shCTL succumbed to leukemic cell burden by 7 and 10 weeks, respectively (Figures 4C and 4D; Figure S4B). In contrast, *p62* knockdown prevented expansion of engrafted leukemic cells and significantly delayed mortality in mice (Figures 4C and 4D). To investigate the cellular effects of p62 depletion in vitro, miR-146a^{low} MDS/AML cell lines and primary del(5q) AML samples were examined for progenitor function, survival, and proliferation. All MDS/AML cell lines with knockdown of *p62* exhibited >80% reduction of leukemic progenitor colonies in methylcellulose ($p < 0.05$ for all) (Figures S4C and S4D). In addition, p62 regulates leukemic cell proliferation, as knockdown of *p62* resulted in delayed growth in vitro, fewer cells in S phase, and accumulation of G0/G1 and G2/M cells (Figure S4E). MDS/AML cell lines with knockdown of *p62* correlated with a significant increase in apoptosis (increased Annexin V^{+} cells; Figure 4E). Loss of p62 did not coincide with a significant increase in apoptosis or changes in cell cycle of control CD34^{+} cells (Figures 4E–4G), suggesting that malignant HSPCs are more sensitive to p62 inhibition. For primary del(5q) MDS/AML cells, knockdown of *p62* also resulted in increased apoptosis (increased Annexin V^{+} cells; Figure 4F; Figure S4F) and suppression of cell cycle (Figure 4G). Despite the differential sensitivity of normal and leukemic cells to *p62* knockdown, treatment with BAY 11-7085 induced apoptosis in both cell types (Figure 4F), revealing that broadly inhibiting NF-κB results in cytotoxicity of normal cells, and as such, the therapeutic limitations of NF-κB inhibitors. Given the role of p62 in regulating autophagy in certain cell types, we examined autophagy in leukemic cells. Notably, knockdown or overexpression of p62 did not change the autophagy status in leukemic cells (Figure S4G).

The p62 signaling domains have been extensively mapped (Moscat and Diaz-Meco, 2009) (Figure 5A). For NF-κB signaling, p62 recruits and activates TRAF6 via its TRAF6-binding (TB) domain (amino acids 228–242), which then results in signaling to IκB kinase (IKK) α/β and NF-κB (Figure 5A) (Seibenhener et al., 2004; Wooten et al., 2005). To determine whether TRAF6 recruitment is essential for p62 function in MDS/AML cells, WT p62 or a mutant p62 lacking the TB domain (p62ΔTB) was coexpressed with shp62. Cell viability was restored in shp62-expressing cells when WT p62 was expressed, but not p62ΔTB, suggesting that interaction with TRAF6 is essential for the effects of p62 in leukemic cells (Figures 5B and 5C). We hypothesized that interfering with the p62-TRAF6 signaling complex in

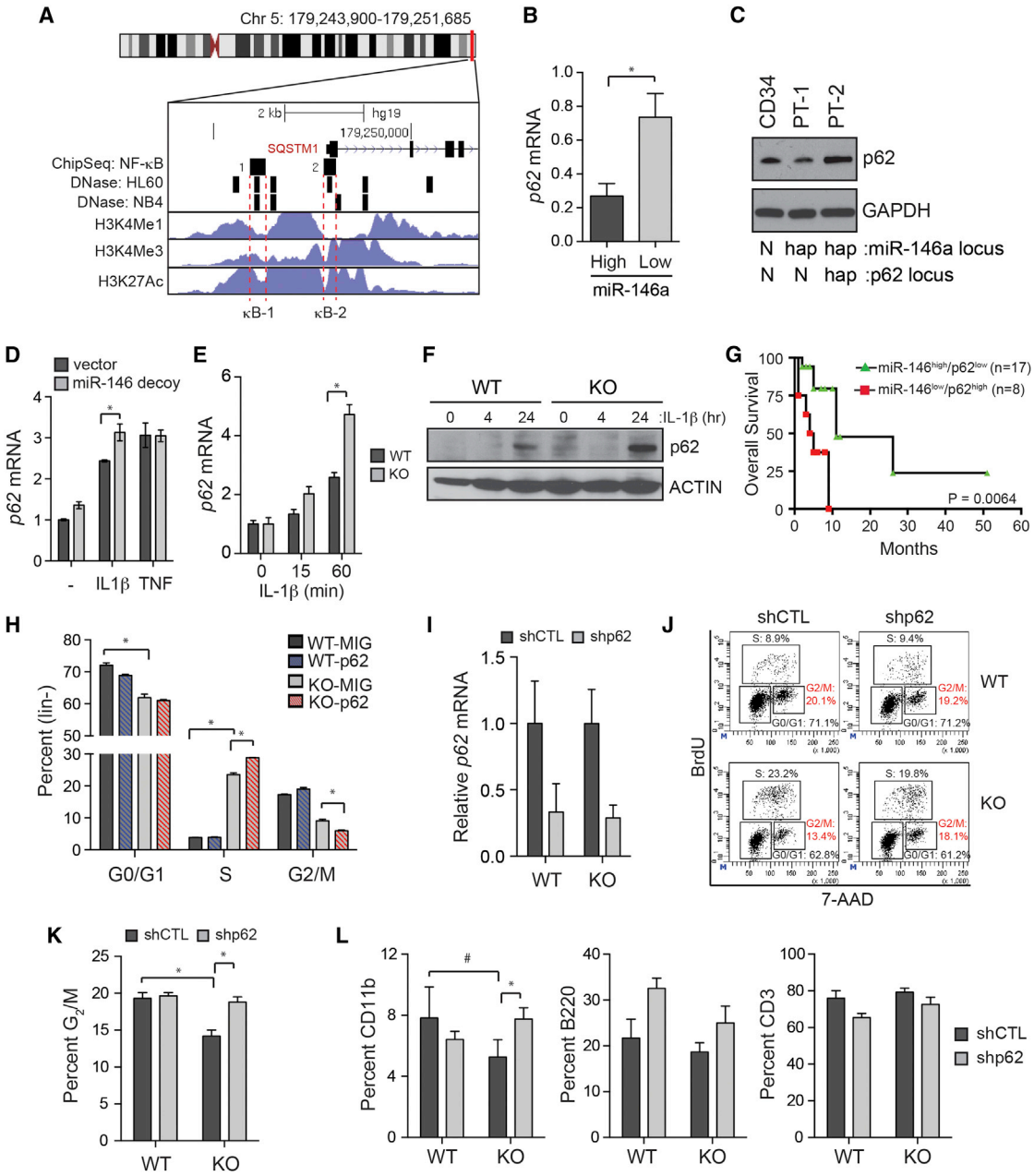

Figure 3. p62 Is Overexpressed through NF-κB Activation and Is an Essential Cofactor in miR-146a$^{-/-}$ HSPCs

(A) Schematic of the *p62* (*SQSTM1*) promoter region. UCSC Genome Browser image displays ENCODE consortium data indicating (top to bottom): location of *SQSTM1* gene (exons depicted as filled boxes, introns as lines with arrows); location of two NF-κB binding regions, based on ChIP-seq data in B cell lines; location of DNase I-hypersensitive regions (indicative of open chromatin) in HL60 and NB4 cells; various histone marks (all indicative of regulatory regions) in K562 cells.

(B) *p62* expression in AML marrow cells with high (top 50th percentile) or low (bottom 50th percentile) miR-146a.

(C) Immunoblot analysis of p62 in del(5q) AML/MDS patient BM cells and normal CD34^{+} cells. The miR-146a and p62 locus status is indicated below (N, normal diploid; hap, haploid).

(D) qRT-PCR expression of *p62* in TF1 leukemic cells transduced with vector or miR-146 decoy and then treated with IL-1β or tumor necrosis factor α.

(E) Quantitative RT-PCR (qRT-PCR) expression of *p62* in HSPC from WT and miR-146$^{-/-}$ mice after treatment with IL-1β at indicated time points.

(F) p62 immunoblot analysis on marrow cells from WT and miR-146$^{-/-}$ mice after treated with IL-1β at indicated time points.

(G) Del(5q) MDS/AML patients were stratified into miR-146a^{high}/p62^{low} and miR-146a^{low}/p62^{high} RNA expression. Overall survival for del(5q) MDS/AML patients based on high miR-146a/low p62 (green, n = 17) and low miR-146a/high p62 (red, n = 8).

(H) Cell-cycle analysis of WT and miR-146a$^{-/-}$ BM transduced with vector (MSCV-IRES-GFP; MIG) or p62.

(I) Validation of *p62* knockdown in WT and miR-146a$^{-/-}$ BM cells by qRT-PCR.

(legend continued on next page)

leukemic cells would be sufficient to inhibit TRAF6-mediated activation of NF-κB and induce cell death and cell-cycle arrest. The TB domain, which consists of 15 amino acids, was fused to a hemagglutinin (HA) epitope tag and then cloned into a retroviral expression vector for sustained expression in leukemic cells. A stop codon (TGA) was inserted following the last amino acid (Lys-242). As a negative control, two critical residues (Phe-232 and Glu-234) were changed to alanine (Figure 5A). Expression of WT (TB^{WT}) and control (i.e., inactive mutant: TB^{MUT}) TB peptide was confirmed by dot blot immunoassay in transduced HL60 and transfected human embryonic kidney 293 (HEK293) cells (Figure 5D). To verify that the WT TB peptide inhibits p62-mediated activation of TRAF6 (as measured by K63-linked autoubiquitination), FLAG-TRAF6 and p62 were cotransfected with TB^{WT} or TB^{MUT} into HEK293 cells followed by immunoprecipitation of TRAF6. TRAF6 autoubiquitination (immunoprecipitation: FLAG; immunoblotting: Ub) was increased following cotransfection of p62, but was then significantly reduced in cells expressing TB^{WT} (Figure 5E). TB^{WT} also suppressed downstream NF-κB signaling as evident by ~25% reduced κB-site reporter gene activation (Figure 5F). To examine the molecular and cellular effects of the TB^{WT} peptide in disease-relevant cells, we transduced HL60 cells with TB^{WT}- and TB^{MUT}-expressing vectors (Figure 5D). Examination of NF-κB activation showed less phosphorylated IKKα/β in TB^{WT}-expressing HL60 cells (Figure 5G). Consistent with suppression of NF-κB/IKK activation, immunoprecipitation of TRAF6 from TB^{WT}-expressing HL60 cells revealed a 50% reduction in ubiquitinated TRAF6, as compared to control (TB^{MUT}) (Figure 5H). Inhibition of TRAF6/NF-κB with TB^{WT} in HL60 cells coincided with impaired G2/M exit (Figure 5I; 26.8% versus 15.2%), apoptosis (Figure 5J; 16.2% versus 3.7%), and impaired leukemic progenitor function (Figure 5K; 144 versus 307 colonies; $p = 0.001$), as compared to normal $CD34^+$ cells. These findings are consistent with the cellular effects observed after depleting p62 (Figures 4E–4G; Figures S4C–S4F). Importantly, TB^{WT} expression also resulted in apoptosis of three independent del(5q) AML patient-derived cells but had no noticeable effect on normal $CD34^+$ cells (Figures 5J–5L). Thus, the TB^{WT} motif exerts antileukemic effects by interfering with TRAF6 and p62 signaling and resulting in cell-cycle arrest, impaired leukemic progenitor function, and increased apoptosis.

DISCUSSION

Several haploinsufficient genes have been identified and verified in the pathogenesis of del(5q) MDS/AML (Ebert, 2009). Despite the progress, our knowledge of genes and gene networks that are necessary for sustaining the del(5q) MDS/AML-propagating cells is insufficiently described. In this study, we show that deletion of miR-146a in del(5q) MDS/AML cells is associated with sustaining the disease phenotype by increasing cell survival and proliferation of the propagating cells through the TRAF6/p62/NF-κB complex. TRAF6 signaling is implicated in del(5q) myeloid malignancies (Starczynowski et al., 2010; Zhao et al., 2013) and an important target in low-risk (LR) MDS (Rhyasen et al., 2013); however, this study uncovers the mechanism by which del(5q) cells have acquired and sustained their dependency on the NF-κB network in HR MDS patients (with elevated blasts) and AML. As part of our effort to uncover del(5q) MDS/AML-specific vulnerabilities and potential therapeutic targets, we identified a subset of 5q genes in which their expression is restored from the intact 5q allele and form an NF-κB signaling node in del(5q) MDS/AML. Furthermore, a detailed promoter analysis confirmed enrichment of NF-κB binding motifs within the promoters of the overexpressed NF-κB node genes, suggesting that an NF-κB feedforward loop exists and may be necessary to sustain the NF-κB signaling pathway following deletion of miR-146a in MDS/AML. *p62*, a key gene within the NF-κB signaling node and an important signaling mediator of TRAF6, is expressed from the intact allele, forming an intrachromosomal gene network with miR-146a to regulate TRAF6 and NF-κB activation (Figure 5M). Importantly, depletion of *p62* has minimal effects on survival, proliferation, or function of normal HSPCs. Although our focus was on p62, we predict that the remaining genes within the NF-κB node are also important for sustaining NF-κB activation (Figure 2). NF-κB is one of the major pathways regulated by activation of TRAF6; however, additional critical pathways regulated by TRAF6 in LR MDS and HR MDS/AML may be different, particularly as they relate to disease initiation versus maintenance. Further investigation into deciphering these molecular pathways during disease evolution and within distinct MDS/AML subtypes is warranted.

Mouse genetic studies have shown that p62 regulates several cellular functions, including bone remodeling, metabolism, and cancer (Linares et al., 2013; Moscat and Diaz-Meco, 2009; Seibenhener et al., 2013). p62 protein contains five signaling and/or interaction modules, including PB1, ZZ-type zinc finger domain (ZZ), TRAF6-binding (TB) domain, LC3-interacting region (LIR), and ubiquitin-associated domain (UBA) (Figure 5A) (Moscat and Diaz-Meco, 2009). Through the TB domain, p62 facilitates K63-linked polyubiquitination of TRAF6 and consequently initiates NF-κB signaling (Sanz et al., 2000). Although the TB domain of p62 has been shown to directly bind TRAF6, overexpression of the TB peptide does not appear to be sufficient to disrupt this interaction in leukemic cells despite efficiently inhibiting p62/TRAF6/NF-κB signaling activity. In our findings, the TB peptide inhibits TRAF6 activation (as measured by TRAF6 autoubiquitination; Figures 5E and 5H) and signaling to NF-κB (Figures 5F and 5G). Collectively, these observations suggest that the TB peptide inhibits p62-mediated activation of TRAF6; however, the mechanism by which TB peptide inhibits TRAF6/NF-κB does not exclusively depend on disrupting the TRAF6-p62 interaction. Nevertheless, we show that the TB peptide exerts antileukemic effects by interfering with TRAF6 and

(J and K) Cell-cycle analysis of WT and miR-146a$^{-/-}$ BM transduced with shCTL or shp62 (J) and summary of replicate experiments (K).
(L) WT and miR-146a$^{-/-}$ HSPCs (CD45.2) transduced with shCTL or shp62 were mixed with 1×10^5 WT (CD45.1) marrow cells and then transplanted into lethally irradiated recipients (n = 8/group). Myeloid and lymphoid proportions in the blood were analyzed 4 weeks posttransplantation.
*$p < 0.05$; #$p < 0.1$. See also Figure S3.

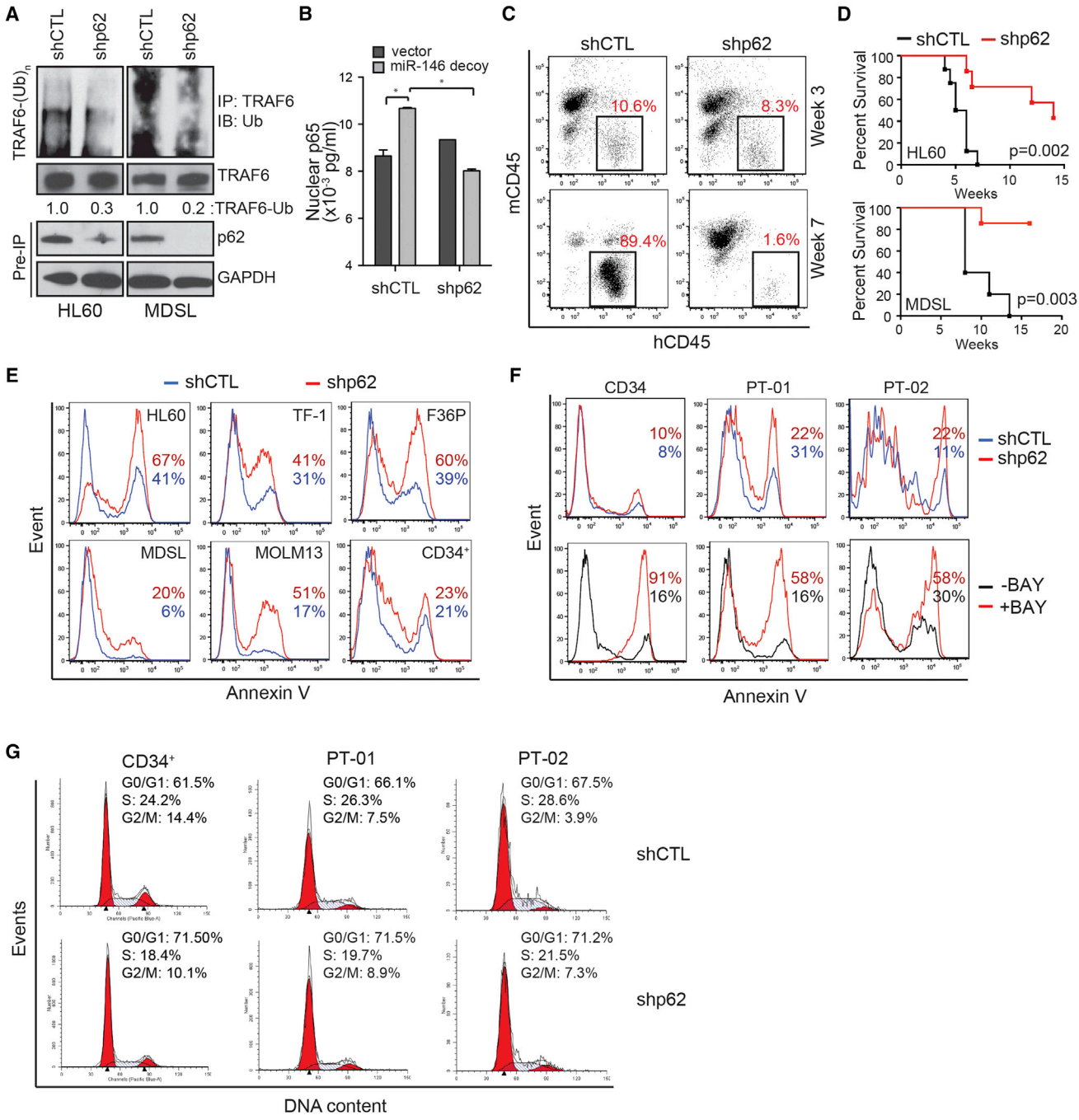

Figure 4. p62 Is Necessary for MDS/AML Cell Survival and Cell Proliferation

(A) *p62* knockdown was confirmed by immunoblotting lysates isolated from cells expressing a control or shp62 lentiviral vector. TRAF6 ubiquitination was measured following transduction with shCTL or shp62.

(B) TF1 cells cotransduced with the indicated vectors were examined for p65 DNA binding.

(C) HL60 cells transduced with shCTL or shp62 were engrafted into NSG mice (n = 5–8/group) and monitored for chimerism at the indicated time points.

(D) Survival curves for mice receiving shCTL- or shp62-transduced HL60 (top) or MDSL (bottom) cells.

(E) Annexin V staining of the indicated cells was determined following transduction with shCTL or shp62.

(F) Annexin V staining of control $CD34^+$ and two del(5q) AML patient samples (PT-01 and PT-02) was determined following transduction with shCTL or shp62. As a positive control, treatment with an NF-κB inhibitor (BAY, BAY 11-7085) resulted in nonspecific cell death.

(G) Cell-cycle analysis of $CD34^+$ and two patient samples (PT-01 and PT-02) transduced with shCTL or shp62 was determined by Hoechst 33342 incorporation.

*$p < 0.05$. See also Figure S4.

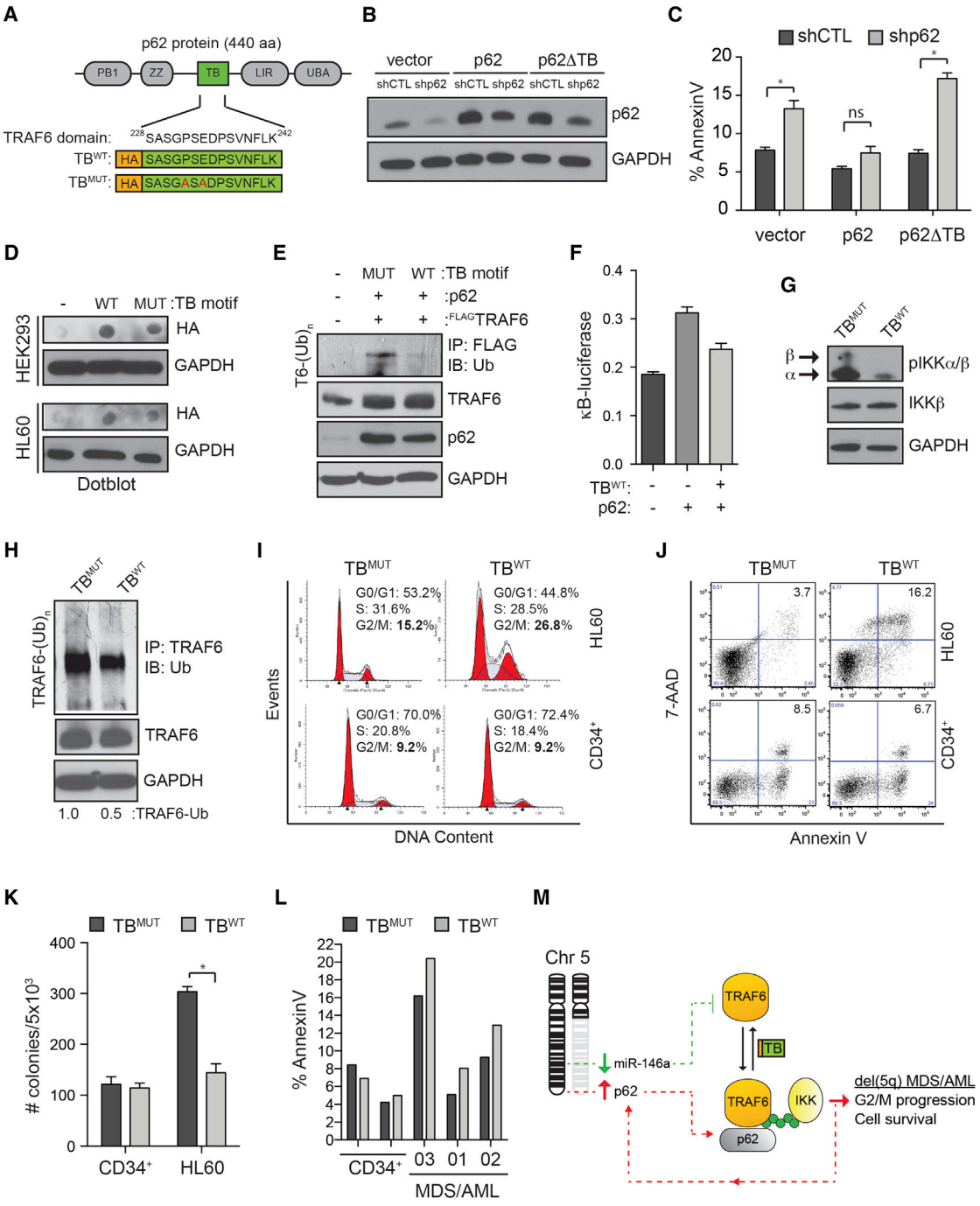

Figure 5. p62 Sustains NF-κB Activation and Leukemic Cell Function via Its TRAF6-Binding Domain

(A) Schematic of the p62 protein and its domains: PB1, ZZ-type zinc finger domain (ZZ), a TRAF6-binding (TB) domain, and LC3-interacting region (LIR), and a ubiquitin-associated domain (UBA). The amino acid sequence of the TB domain and the schematic of a WT and mutant TB constructs are shown below.

(B and C) HL60 expressing MIG, MIG-p62, or MIG-p62ΔTB retroviral vectors were transduced with shCTL or shp62. p62 expression (B) and cell survival (C) was analyzed 4 days posttransduction.

(D) Expression of empty vector (MSCV-pGK-GFP), TB^{Mut}, or TB^{WT} by transient transfection in HEK293 or by transduction in HL60 was confirmed by dot blot immunoassay.

(E) HEK293 cells transfected with the indicated constructs were analyzed by coimmunoprecipitation and immunoblotting.

(F) NF-κB activation was measured in HEK293 cells transfected with a κB site-luciferase and the indicated vectors (n = 3/group). Values represent κB-site firefly over *Renilla* luciferase.

(G) IKKα/β phosphorylation was measured in HL60 cells transduced with TB^{Mut} or TB^{WT} by immunoblotting.

(legend continued on next page)

p62 signaling and resulting in cell-cycle arrest, impaired leukemic progenitor function, and increased apoptosis. An essential role of p62 in cancer-associated TRAF6/NF-κB has been also described in solid tumors (Beg et al., 1995; Duran et al., 2008). In one of these studies, p62 is required for RAS to activate IKK through polyubiquitination of TRAF6 in lung adenocarcinomas. In normal and RAS-transformed cells, p62 controls timely transit of cells through mitosis and tumor cell proliferation (Linares et al., 2011). These previous findings are consistent with our observation that p62 is important for increased cell proliferation and G2/M transition in miR-146a^{low}-expressing leukemic cells. Selectively inhibiting TRAF6 has not been feasible, as it does not possess druggable protein interfaces; therefore, interfering with the p62-TRAF6 interaction may be a novel therapeutic option, particularly in miR-146a^{low}-expressing leukemia. Similar approaches using a deliverable peptide to prevent protein interactions have been proposed and successfully implemented in human cancer (Thundimadathil, 2012).

Since del(5q) MDS/AML is associated with a variety of other cytogenetic changes, for this study we focused on differentially expressed genes residing within chr5. A focused analysis examining just chr5q genes allowed for a simpler interpretation while providing a proof of concept that intra- and/or interchromosomal gene networks may expose therapeutic vulnerabilities. Two recent studies have proposed that passenger deletions, which in certain cancers involve functionally redundant gene families or necessary housekeeping genes, create therapeutic vulnerabilities (Muller et al., 2012; Nijhawan et al., 2012). This concept is exemplified by the restored expression of p62 from the intact chr5q allele in order to sustain NF-κB signaling by recruiting TRAF6 in miR-146a-deficient HSPCs (Figure 5M). Del(5q) MDS/AML patients with low miR-146a expression nearly always have normal/elevated p62, highlighting the pathologic connection between miR-146a and p62. In addition, this study reinforces synthetic dependencies based on intrachromosomal gene networks associated with a specific genomic alteration. Although our findings revealed an important role of p62 in sustaining NF-κB-mediated proliferation and survival pathways in HR del(5q) MDS/AML, based on p62 knockdown experiments, we also anticipate that p62 will similarly sustain NF-κB signaling in non-del(5q) AML cells with low miR-146a expression. Not all NF-κB-target genes are overexpressed in del(5q) MDS as one might have expected following deletion of miR-146a (Figure S2C). This observation suggests that there is selective regulation of certain NF-κB-target genes, such as the ones described as part of the intrachromosomal network within chr5 (Figures 2A and 2B). Lastly, we also postulate that non-chr5 genes may equally contribute to the del(5q) network and that intra- and interchromosomal gene networks may expose therapeutic vulnerabilities in MDS/AML with other cytogenetic alterations (i.e., monosomy 7).

EXPERIMENTAL PROCEDURES

See Supplemental Experimental Procedures for additional information.

Mice and Primary Murine Bone Marrow Cell Culture

Animals were bred and housed in the Association for Assessment and Accreditation of Laboratory Animal Care-accredited animal facility of Cincinnati Children's Hospital Medical Center. Whole-body miR-146a$^{-/-}$ mice were a kind gift from Dr. Dinesh Rao (University of California, Los Angeles). All experiments were carried out under approved animal protocols by the Cincinnati Children's Hospital Institutional Animal Committee. BM cells were obtained by crushing the femur, tibia, and pelvic bone into RPMI 1640 containing 2% bovine serum, 1% penicillin-streptomycin, and 1 mM EDTA and then filtered through a 40 μm cell strainer. The cells were maintained in RPMI 1640 supplemented with 10% fetal bovine serum, 1% penicillin-streptomycin, recombinant mouse stem cell factor (rmSCF; 02931, STEMCELL Technologies), mouse interleukin 3 (rmIL-3; 02903, STEMCELL Technologies), and human interleukin 6 (rhIL-6; 02606, STEMCELL Technologies) at 10 ng/ml.

Patient Samples

Informed consent was obtained according to protocols approved by the review boards of Cleveland Clinics. Diagnoses were reviewed at Cleveland Clinics and adapted, when required, to World Health Organization 2008 criteria. For quantitative RT-PCR analysis, bone marrow aspirates were collected from 41 patients and 15 age-matched healthy controls (Table S1). For functional studies, MDS/AML peripheral mononuclear cells (Table S1) were cultured in StemSpan serum-free expansion media (SFEM; STEMCELL Technologies) supplemented with 100 ng/ml recombinant human stem cell factor (rhSCF; 02830, STEMCELL Technologies), human Flt3 ligand (rhFL; 02840, STEMCELL Technologies), and human thrombopoietin (rhTPO; 02522, PeproTech) for 48 hr before transduction. Cells were cultured in rhSCF, rhFlt3L, rhTPO, rhIL-3, and rhIL-6 at 10 ng/ml.

Transcription Factor Bioinformatic Analysis

To identify TFs that might be regulating the compensated genes on chr5q, we searched for enriched TF binding motifs in their promoter regions. For each gene, we defined the promoter region as the 1,000 bases upstream of the start of the longest gene transcript, as annotated in the RefSeq database (Pruitt et al., 2009). We compiled a total of 1,867 TF binding motif models (in the form of position weight matrices) from Transfac (Matys et al., 2006), JASPAR (Portales-Casamar et al., 2010), FactorBook (Wang et al., 2013), UniProbe (Robasky and Bulyk, 2011), hmCHIP (Chen et al., 2011), and Jolma (Jolma et al., 2013), which in total cover 623 distinct human TFs. We then used the Pscan software package (Zambelli et al., 2009) to rank all TF motifs based on their enrichment in the chr5q gene set, as compared to random expectation based on background distributions obtained by scanning all RefSeq promoters.

(H) TRAF6 ubiquitination (TRAF6 immunoprecipitaion; Ub immunoblotting) was measured in HL60 transduced with TB^{Mut} and TB^{WT}.
(I) Cell-cycle analysis of HL60 and CD34$^+$ cells transduced with TB^{Mut} or TB^{WT} was determined by Hoechst 33342 incorporation.
(J) Annexin V staining of HL60 and control CD34$^+$ cells was determined following transduction with TB^{Mut} or TB^{WT}.
(K) HL60 and CD34$^+$ cells were transduced with TB^{Mut} or TB^{WT} and then plated in methylcellulose for progenitor colony formation (n = 3/group). Colonies were scored 10–14 days after plating.
(L) Annexin V staining of control CD34$^+$ cells and MDS/AML patient samples (PT-01, PT-02, and PT-03) was determined following transduction with TB^{Mut} or TB^{WT}.
(M) Model of an intrachromosomal network involving miR-146a/p62/TRAF6/NF-κB in HR del(5q) MDS/AML. miR-146a deletion results in derepression of TRAF6 protein. TRAF6 overexpression results in its autoubiquitination (green circles), which serves to recruit and then activate the NF-κB kinase complex (IKKα/β). NF-κB transcription factors induce p62/SQSTM1 expression from the remaining allele within del(5q). p62 is an important cofactor to sustain NF-κB activation through its TRAF6-binding domain (TB). The p62/TRAF6 signaling complex and subsequent NF-κB activation can be inhibited by expressing the TB motif.
*$p < 0.05$.

Statistical Analysis

Results are depicted as the mean ± SEM. Statistical analyses were performed using Student's t test. For microarray data, Benjamini Hochberg correction was applied based on the total number of gene expression probes analyzed for the region. Probes with an adjusted p value ≤ 0.05 were considered significant (Table S2). GraphPad Prism (v5, GraphPad) was used for statistical analysis.

ACCESSION NUMBERS

The GEO accession number for the microarray data reported in this paper is GSE60649.

SUPPLEMENTAL INFORMATION

Supplemental Information includes Supplemental Experimental Procedures, four figures, and three tables and can be found with this article online at http://dx.doi.org/10.1016/j.celrep.2014.07.062.

ACKNOWLEDGMENTS

This work was supported by the Cincinnati Children's Hospital Research Foundation, the American Society of Hematology (ASH), the NIH (RO1HL111103), Gabrielle's Angel Foundation, and the Department of Defense grants (to D.T.S.). The umbilical cord blood samples were received through the Normal Donor Repository in the Translational Core Laboratory at Cincinnati Children's Research Foundation, which is supported through the NIDDK Center's of Excellence in Experimental Hematology (P30DK090971). We thank the Mt. Auburn Ob-Gyn associates and delivery nursing staff at Christ Hospital, Cincinnati, for collecting cord blood ($CD34^+$) samples from normal deliveries. We thank Jeff Bailey and Victoria Summey for assistance with transplantations and xenotransplantations (Comprehensive Mouse and Cancer Core). MDSL cells were kindly provided by Dr. Kaoru Tohyama. We thank Dr. Ruhikanta Meetei for technical recommendations.

Received: September 11, 2013
Revised: June 5, 2014
Accepted: July 31, 2014
Published: September 4, 2014

REFERENCES

Beg, A.A., Sha, W.C., Bronson, R.T., and Baltimore, D. (1995). Constitutive NF-kappa B activation, enhanced granulopoiesis, and neonatal lethality in I kappa B alpha-deficient mice. Genes Dev. *9*, 2736–2746.

Boldin, M.P., Taganov, K.D., Rao, D.S., Yang, L., Zhao, J.L., Kalwani, M., Garcia-Flores, Y., Luong, M., Devrekanli, A., Xu, J., et al. (2011). miR-146a is a significant brake on autoimmunity, myeloproliferation, and cancer in mice. J. Exp. Med. *208*, 1189–1201.

Chen, F.E., Huang, D.B., Chen, Y.Q., and Ghosh, G. (1998). Crystal structure of p50/p65 heterodimer of transcription factor NF-kappaB bound to DNA. Nature *391*, 410–413.

Chen, J., Bardes, E.E., Aronow, B.J., and Jegga, A.G. (2009). ToppGene Suite for gene list enrichment analysis and candidate gene prioritization. Nucleic Acids Res. *37*, W305–W311.

Chen, L., Wu, G., and Ji, H. (2011). hmChIP: a database and web server for exploring publicly available human and mouse ChIP-seq and ChIP-chip data. Bioinformatics *27*, 1447–1448.

Duran, A., Linares, J.F., Galvez, A.S., Wikenheiser, K., Flores, J.M., Diaz-Meco, M.T., and Moscat, J. (2008). The signaling adaptor p62 is an important NF-kappaB mediator in tumorigenesis. Cancer Cell *13*, 343–354.

Ebert, B.L. (2009). Deletion 5q in myelodysplastic syndrome: a paradigm for the study of hemizygous deletions in cancer. Leukemia *23*, 1252–1256.

Giagounidis, A.A., Germing, U., and Aul, C. (2006). Biological and prognostic significance of chromosome 5q deletions in myeloid malignancies. Clin. Cancer Res. *12*, 5–10.

Greenberg, P.L., Tuechler, H., Schanz, J., Sanz, G., Garcia-Manero, G., Solé, F., Bennett, J.M., Bowen, D., Fenaux, P., Dreyfus, F., et al. (2012). Revised international prognostic scoring system for myelodysplastic syndromes. Blood *120*, 2454–2465.

Jerez, A., Gondek, L.P., Jankowska, A.M., Makishima, H., Przychodzen, B., Tiu, R.V., O'Keefe, C.L., Mohamedali, A.M., Batista, D., Sekeres, M.A., et al. (2012). Topography, clinical, and genomic correlates of 5q myeloid malignancies revisited. J. Clin. Oncol. *30*, 1343–1349.

Jolma, A., Yan, J., Whitington, T., Toivonen, J., Nitta, K.R., Rastas, P., Morgunova, E., Enge, M., Taipale, M., Wei, G., et al. (2013). DNA-binding specificities of human transcription factors. Cell *152*, 327–339.

Komurov, K., Dursun, S., Erdin, S., and Ram, P.T. (2012). NetWalker: a contextual network analysis tool for functional genomics. BMC Genomics *13*, 282.

Linares, J.F., Amanchy, R., Greis, K., Diaz-Meco, M.T., and Moscat, J. (2011). Phosphorylation of p62 by cdk1 controls the timely transit of cells through mitosis and tumor cell proliferation. Mol. Cell. Biol. *31*, 105–117.

Linares, J.F., Duran, A., Yajima, T., Pasparakis, M., Moscat, J., and Diaz-Meco, M.T. (2013). K63 polyubiquitination and activation of mTOR by the p62-TRAF6 complex in nutrient-activated cells. Mol. Cell *51*, 283–296.

Ling, J., Kang, Y., Zhao, R., Xia, Q., Lee, D.F., Chang, Z., Li, J., Peng, B., Fleming, J.B., Wang, H., et al. (2012). KrasG12D-induced IKK2/β/NF-κB activation by IL-1α and p62 feedforward loops is required for development of pancreatic ductal adenocarcinoma. Cancer Cell *21*, 105–120.

List, A., Dewald, G., Bennett, J., Giagounidis, A., Raza, A., Feldman, E., Powell, B., Greenberg, P., Thomas, D., Stone, R., et al.; Myelodysplastic Syndrome-003 Study Investigators (2006). Lenalidomide in the myelodysplastic syndrome with chromosome 5q deletion. N. Engl. J. Med. *355*, 1456–1465.

Matys, V., Kel-Margoulis, O.V., Fricke, E., Liebich, I., Land, S., Barre-Dirrie, A., Reuter, I., Chekmenev, D., Krull, M., Hornischer, K., et al. (2006). TRANSFAC and its module TRANSCompel: transcriptional gene regulation in eukaryotes. Nucleic Acids Res. *34*, D108–D110.

Moscat, J., and Diaz-Meco, M.T. (2009). p62 at the crossroads of autophagy, apoptosis, and cancer. Cell *137*, 1001–1004.

Muller, F.L., Colla, S., Aquilanti, E., Manzo, V.E., Genovese, G., Lee, J., Eisenson, D., Narurkar, R., Deng, P., Nezi, L., et al. (2012). Passenger deletions generate therapeutic vulnerabilities in cancer. Nature *488*, 337–342.

Nijhawan, D., Zack, T.I., Ren, Y., Strickland, M.R., Lamothe, R., Schumacher, S.E., Tsherniak, A., Besche, H.C., Rosenbluh, J., Shehata, S., et al. (2012). Cancer vulnerabilities unveiled by genomic loss. Cell *150*, 842–854.

Portales-Casamar, E., Thongjuea, S., Kwon, A.T., Arenillas, D., Zhao, X., Valen, E., Yusuf, D., Lenhard, B., Wasserman, W.W., and Sandelin, A. (2010). JASPAR 2010: the greatly expanded open-access database of transcription factor binding profiles. Nucleic Acids Res. *38*, D105–D110.

Pruitt, K.D., Tatusova, T., Klimke, W., and Maglott, D.R. (2009). NCBI Reference Sequences: current status, policy and new initiatives. Nucleic Acids Res. *37*, D32–D36.

Rhyasen, G.W., Bolanos, L., Fang, J., Jerez, A., Wunderlich, M., Rigolino, C., Mathews, L., Ferrer, M., Southall, N., Guha, R., et al. (2013). Targeting IRAK1 as a therapeutic approach for myelodysplastic syndrome. Cancer Cell *24*, 90–104.

Robasky, K., and Bulyk, M.L. (2011). UniPROBE, update 2011: expanded content and search tools in the online database of protein-binding microarray data on protein-DNA interactions. Nucleic Acids Res. *39*, D124–D128.

Rosenbloom, K.R., Sloan, C.A., Malladi, V.S., Dreszer, T.R., Learned, K., Kirkup, V.M., Wong, M.C., Maddren, M., Fang, R., Heitner, S.G., et al. (2013). ENCODE data in the UCSC Genome Browser: year 5 update. Nucleic Acids Res. *41*, D56–D63.

Sanz, L., Diaz-Meco, M.T., Nakano, H., and Moscat, J. (2000). The atypical PKC-interacting protein p62 channels NF-kappaB activation by the IL-1-TRAF6 pathway. EMBO J. *19*, 1576–1586.

Seibenhener, M.L., Babu, J.R., Geetha, T., Wong, H.C., Krishna, N.R., and Wooten, M.W. (2004). Sequestosome 1/p62 is a polyubiquitin chain binding protein involved in ubiquitin proteasome degradation. Mol. Cell. Biol. *24*, 8055–8068.

Seibenhener, M.L., Du, Y., Diaz-Meco, M.T., Moscat, J., Wooten, M.C., and Wooten, M.W. (2013). A role for sequestosome 1/p62 in mitochondrial dynamics, import and genome integrity. Biochim. Biophys. Acta *1833*, 452–459.

Starczynowski, D.T., Kuchenbauer, F., Argiropoulos, B., Sung, S., Morin, R., Muranyi, A., Hirst, M., Hogge, D., Marra, M., Wells, R.A., et al. (2010). Identification of miR-145 and miR-146a as mediators of the 5q- syndrome phenotype. Nat. Med. *16*, 49–58.

Starczynowski, D.T., Morin, R., McPherson, A., Lam, J., Chari, R., Wegrzyn, J., Kuchenbauer, F., Hirst, M., Tohyama, K., Humphries, R.K., et al. (2011). Genome-wide identification of human microRNAs located in leukemia-associated genomic alterations. Blood *117*, 595–607.

Taganov, K.D., Boldin, M.P., Chang, K.J., and Baltimore, D. (2006). NF-kappaB-dependent induction of microRNA miR-146, an inhibitor targeted to signaling proteins of innate immune responses. Proc. Natl. Acad. Sci. USA *103*, 12481–12486.

Thundimadathil, J. (2012). Cancer treatment using peptides: current therapies and future prospects. J. Amino Acids *2012*, 967347.

Wang, J., Zhuang, J., Iyer, S., Lin, X.Y., Greven, M.C., Kim, B.H., Moore, J., Pierce, B.G., Dong, X., Virgil, D., et al. (2013). Factorbook.org: a Wiki-based database for transcription factor-binding data generated by the ENCODE consortium. Nucleic Acids Res. *41*, D171–D176.

Wooten, M.W., Geetha, T., Seibenhener, M.L., Babu, J.R., Diaz-Meco, M.T., and Moscat, J. (2005). The p62 scaffold regulates nerve growth factor-induced NF-kappaB activation by influencing TRAF6 polyubiquitination. J. Biol. Chem. *280*, 35625–35629.

Zambelli, F., Pesole, G., and Pavesi, G. (2009). Pscan: finding over-represented transcription factor binding site motifs in sequences from co-regulated or co-expressed genes. Nucleic Acids Res. *37*, W247–W252.

Zhao, J.L., Rao, D.S., Boldin, M.P., Taganov, K.D., O'Connell, R.M., and Baltimore, D. (2011). NF-kappaB dysregulation in microRNA-146a-deficient mice drives the development of myeloid malignancies. Proc. Natl. Acad. Sci. USA *108*, 9184–9189.

Zhao, J.L., Rao, D.S., O'Connell, R.M., Garcia-Flores, Y., and Baltimore, D. (2013). MicroRNA-146a acts as a guardian of the quality and longevity of hematopoietic stem cells in mice. Elife (Cambridge) *2*, e00537.